Lumley, J. L., "Drag Reduction by Additives," *Ann. Rev. Fluid Mech.*, 1, 369 (1969).
Marrucci, G., and G. Astarita, "Turbulent Heat Transfer in Viscoelastic Liquids," *Ind. Eng. Chem. Fundamentals*, 6, 470 (1967).
McConaghy, G. A., "The Effect of Drag Reducing Polymers on Turbulent Mass Transfer," Ph.D. thesis, Univ. Ill., Urbana (1974).
McNally, W. A., "Heat and Momentum Transport in Dilute Polyethylene Oxide Solutions," *Naval Underwater Weapons Research and Engineering Station TR No. 44* (1968).
Meyer, W. A., "A Correlation of the Frictional Characteristics for Turbulent Flow of Dilute Viscoelastic Non-Newtonian Fluids in Pipes," *AIChE J.*, 12, 522 (1966).
Newson, J. D., and A. C. Riddiford, "Limiting Currents for the Reduction of the Tri-iodide Ion at a Rotating Platinum Disk Cathode," *J. Electrochem. Soc.*, 103, 695 (1961)
Poreh, M., and V. Paz, "Turbulent Heat Transfer to Dilute Polymer Solutions," *Intern. J. Heat Mass Transfer*, 11, 805 (1969).
Reischman, M. M., "Laser Anemometer Measurements in Drag-Reducing Channel Flows," Ph.D. thesis, Okla. State Univ., Stillwater (1973).
Shaw, D. A., "Mechanism of Turbulent Mass Transfer to a Pipe Wall at High Schmidt Numbers," Ph.D. thesis, Univ. Ill., Urbana (1976).
Sidahmed, G. H., and R. G. Griskey, "Mass Transfer in Drag Reducing Fluid Systems," *AIChE J.*, 18, 138 (1972).
Smith, K. A., G. H. Keuroghlian, P. S. Virk, and E. W. Merril, "Heat Transfer to Drag-Reducing Solutions," *ibid.*, 15, 294 (1969).
Son, J. S., and T. J. Hanratty, "Limiting Relation for Eddy Diffusivity Close to a Wall," *ibid.*, 13, 689 (1967).
Van Shaw, P., Ph.D. thesis, "A Study of the Fluctuations and the Time Average of the Rates of Mass Transfer to a Pipe Wall," Univ. Ill., Urbana (1963).
Wells, C. S., ed., *Viscous Drag Reduction*, Plenum Press, New York (1969).

Manuscript received September 17, 1976; revision received March 28, and accepted March 30, 1977.

Crystal Size Distribution Dynamics in a Classified Crystallizer:

Part I. Experimental and Theoretical Study of Cycling in a Potassium Chloride Crystallizer

ALAN D. RANDOLPH
JAMES R. BECKMAN
and
ZLATICA I. KRALJEVICH

Department of Chemical Engineering
University of Arizona
Tucson, Arizona 85721

Cycles in particle size and slurry density were experimentally observed in a mixed suspension, potassium chloride crystallizer equipped with a fines dissolver and having nonrepresentative product withdrawal. Cycling behavior was achieved with a product crystal elutriator but was also observed with changes in the orientation of the product removal tube, indicating that instability was induced by product classification. Simulation of the unstable runs with a dynamic model showed crystal size distribution (CSD) limit cycles of similar period using nucleation kinetics and process conditions measured experimentally. The computer simulation showed no tendency towards cycling for the stable runs.

SCOPE

CSD is an important property of an operating crystallizer. Much effort has been spent in reducing CSD transients and eliminating CSD instability in industrial crystallizers in order to make a product within the desired size range at the desired production. Extreme CSD cycling can cause production losses due to off-specification product, overload of dewatering equipment, and exacerbated equipment fouling. Transients of CSD are caused by outside crystallizer upsets (for example, dilution addition, feed rate or composition change, interior fouling, etc.), while unstable CSD's result from the interaction of the system kinetics with the particular crystallizer configuration. The present study demonstrates, both experimentally and theoretically, the phenomenon of low-order cycling wherein CSD instability is caused by the crystallizer configuration (fines destruction and classified product removal) in a stable low-order region of nucleation vs. supersaturation response.

Correspondence should be directed to Dr. Randolph. James R. Beckman is at California State University, Northridge, California.

CONCLUSIONS AND SIGNIFICANCE

Significant product classification together with fines destruction were shown to cause cycling of CSD in a mixed suspension crystallizer. This result was demonstrated both experimentally and by numerical simulation. Such instability can occur even in an insensitive region of nucleation behavior; however, the amplitude of the CSD limit cycles depends upon the nucleation sensitivity as well as the sizes and rates at which fines removal and product classification are occurring. Sufficient classification to cause cycling was obtained in this experimental study either with a product crystal elutriator or nonisokinetic slurry withdrawal. In general, crystallizer configuration and operation to produce large crystals with a narrow distribution exacerbates the tendency toward cycling. The factors causing the low-order cycling observed in this study are probably similar to the causes of instability in industrial crystallizers.

Much elegant analytical work has been done on the problem of predicting crystallizer instability. These analytical studies have revealed two types of CSD instability, high and low-order cycling, having the following attributes:

High-order cycling

1. CSD cycles around the exponential MSMPR distribution. Cycling can occur with or without fines dissolving.
2. Stability criterion is of the form

$$\frac{d(\log B)}{d(\log G)} < I(g) - \lambda$$

where $I(\infty) = 21$ for the Class II (high yield) crystallizer and λ is the exponential decay factor for population density due to fines removal.

3. Stability depends greatly on the form of nucleation kinetics.
4. Cycling is only predicted to occur with high-order relationship of nucleation to supersaturation, for example, nucleation discontinuity.
5. Volmer and Miers nucleation models predict cycling for small values of supersaturation, for example, at long retention times.
6. Instability can occur at high supersaturations if a new mechanism creates sudden nucleation discontinuity.

References: Hulburt and Stefango, (1969), Lei et al., (1971), Randolph and Larson, Chapt. 5 (1971), Randolph and Larson (1965).

Low-order cycling

1. Caused mainly by nonrepresentative product removal.
2. CSD cycles around a narrower distribution than the wide MSMPR form.
3. Cycling is not a strong function of the form of nucleation kinetics and occurs with low-order power law kinetics commonly measured in mixed suspension crystallizers.
4. Combined fines destruction and classified product removal exacerbates tendency to cycle.
5. Has been observed in industrial inorganic crystallizers of complex configuration, for example, fines removal, clear liquor advance, and product classification

References: Randolph et al. (1973), Sherwin et al. (1967), Randolph and Larson, Chapt. 5 (1971).

A recent publication (Randolph et al., 1973) analyzes the phenomenon of low-order cycling in crystallizers of complex configuration having fines destruction, nonrepresentative product removal, and clear liquor advance with nucleation given by a secondary magma dependent formulation. This study conclusively demonstrated the possibility of cycling in such systems having low-order kinetic nucleation behavior, for example, the power law nucleation kinetics commonly obtained by correlation of MSMPR data. All that is needed to produce cycling is to have significant product classification in a size approaching the mean size of the CSD in suspension. Such classification in large equipment can easily occur owing to nonrepresentative product removal at the point of slurry discharge. Cycling tendency is exacerbated by fines destruction and clear liquor advance.

Figure 1 plots CSD data from an industrial potassium chloride crystallizer. (Such cycling is not normal in this particular unit but was caused by abnormal operating conditions that brought about a larger effective fines removal rate.) Note the long cycle period of about 24 hr and the progression of crystal disturbances down the size axis. These peaks progress with an average crystal growth velocity of about 0.9 μm/min. Production rate and slurry density are perturbed as such CSD cycles pass through the system.

In the present experimental and theoretical study we had two goals. First, to produce CSD cycling in a well-documented, bench scale crystallizer of complex configuration (fines destruction, classified product, clear liquor advance) as commonly used industrially. Second, to analyze CSD cycling from this system with a numerical computer simulation so that causes and cures of instability could be better understood. In Part II we consider control schemes that might stabilize CSD or minimize the effects of cyclic behavior.

THEORETICAL CONSIDERATIONS

The stability criterion for a class II (high yield) MSMPR crystallizer with a point fines dissolving system

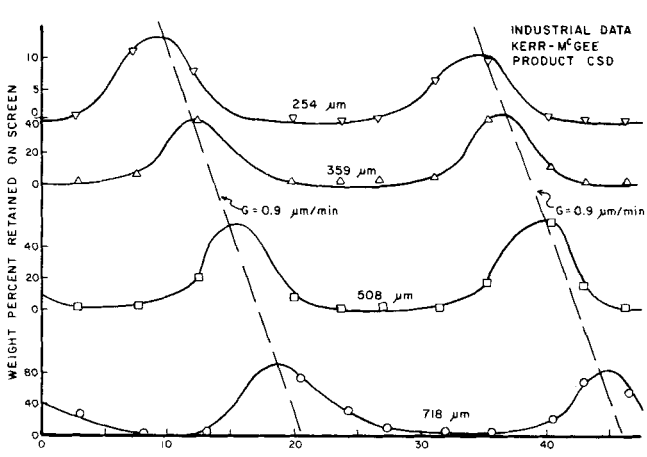

Fig. 1. Unstable crystal size distribution behavior in an industial KCl crystallizer [Courtesy Kerr-McGee Corporation, Trona, CA].

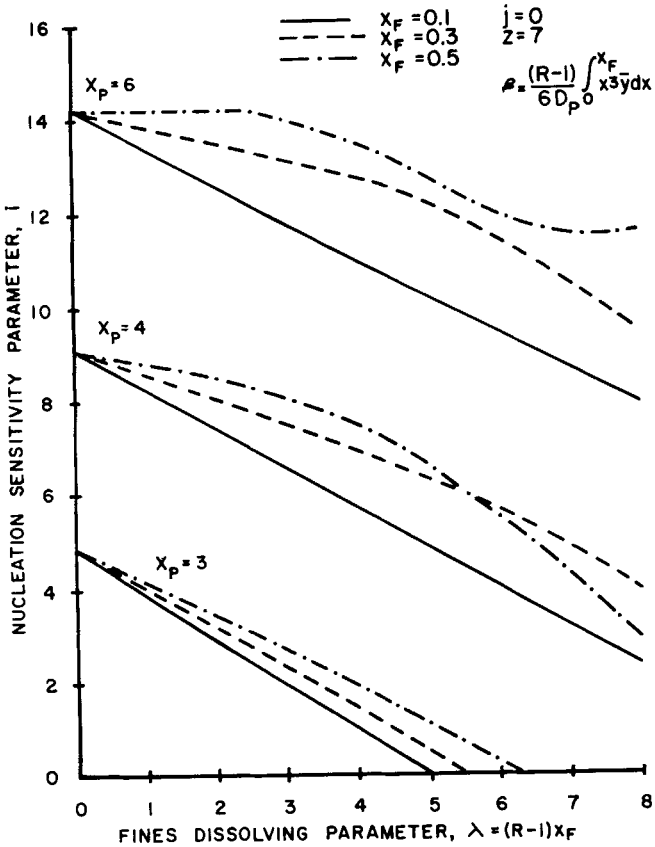

Fig. 2. Crystallizer stability for the R-z crystallizer with fines destruction and classified produce removal (Magma-independent Nucleation) [After Randolph, *et al.*, 1973].

(negligible mass dissolved) is given simply as

$$\frac{d(\log B^o)}{d(\log G)} < I(\infty) - \lambda \qquad (1)$$

where

$$I(\infty) = 21$$

$\lambda = L_F Q_F / GV$ is the exponential decay factor of originally formed nuclei. This parameter can typically range from 2 to 7 in industrial systems.

This result is derived simply from a linearized stability analysis of the first three moments of the population density (Randolph and Larson, Chapt. 5, 1971). For a class I (variable yield) system, the stability criterion is somewhat relaxed to

$$\frac{d(\log B^o)}{d(\log G)} < I(g) - \lambda \qquad (2)$$

where $I(g)$ undergoes a minimum of about 11 to 12 for yields $[C - C_s]/[C_i - C_s]$ of about 50%. Such low per pass yields are unacceptable in most industrial processes; the system is usually modified to increase yields (for example, clear liquor advance) which forces the system towards class II behavior.

The effect of fines destruction, with appreciable mass dissolved, in a class II MSMPR system is to stabilize CSD. Thus, for such systems

$$\frac{d(\log B^o)}{d(\log G)} \gtrless 21 - \lambda + f(\text{fines size and mass}) \qquad (3)$$

for instability to occur (Lei et al., 1971; Randolph et al., 1973).

This indicates that fines dissolving per se is not the cause of cycling in systems which exhibit normal low-order modes of secondary nucleation. Equations (1) to (3) indicate that for CSD to cycle in such MSMPR systems, an essentially discontinuous high-order relationship must exist between nucleation and growth rate. The Miers nucleation/growth rate model given as

$$\left.\begin{aligned} B^o &= k_N (C - C_m)^i \\ G &= k_g (C - C_s) \end{aligned}\right\} \; C_m > C_s \qquad (4)$$

exhibits such high-order behavior as the concentration drops towards the metastable limit C_m. The stability criterion for such systems is given as

$$\frac{d(\log B^o)}{d(\log G)} = i\frac{[C - C_s]}{[C - C_m]} < I(g) - \lambda \qquad (5)$$

Obviously, as $C \to C_m$, this stability criterion is violated even for low values of the power law kinetics parameter i.

Miers model nucleation kinetics represent a linearization of the complex Volmer model; such expressions have been successfully applied to the description of nucleation behavior in a class I system (Song et al., 1975). Their system could be made to cycle around the MSMPR distribution as the retention time was increased, forcing $C \to C_m$.

On the other hand, product classification at a size approaching the mean (weight averaged) size of the CSD in suspension severely destabilizes the system and can result in the phenomenon of low-order CSD cycling. That is, the CSD will cycle in a region where nucleation rate is given as a low-order kinetic function of the supersaturation driving force; such low-order kinetics are typical of most heavy magma crystallizers in which nucleation is by secondary mechanisms. Sherwin et al. (1969) first illustrated the dramatic effect on stability of product classification, although they used an unrealistic Volmer nucleation model and a highly idealized classification model. In a recent study (Randolph et al., 1973), the combination of product classification, fines destruction, and clear liquor advance were shown to result in low-order CSD cycling with the secondary nucleation kinetics and complex configurations common in industrial practice. In their study, size dependent removal rate due to fines destruction and nonrepresentative product removal was modeled as

$$Q(L)/Q = h(L) = \begin{cases} R, & L < L_F \\ 1, & L \text{ in } (L_F, L_P) \\ z, & L > L_P \end{cases} \qquad (6)$$

Thus, removal rate of fines and oversize are respectively R and z times the mixed removal rate Q. This so-called R-z crystallizer model is a useful design concept for industrial crystallizers (Randolph and Larson, Chapt. 8, 1971) and captures the essence of the CSD behavior of crystallizers with complex configuration. Figure 2 (Randolph et al., 1973) shows the interaction between fines destruction and product classification which aggravates the tendency towards cycling. The effect of clear liquor advance is to lower the mixed discharge rate Q, thus magnifying the effects of both fines destruction and classification.

Figure 2 illustrates that low-order cycling could occur in such a crystallizer with relatively insensitive nucleation behavior, that is, power law nucleation exponent in the range $i = 1$ to 5 as typically observed from MSMPR kinetics studies. The amount and size range of product classification required to produce instability is such that low-order cycling could result from nonrepresentative removal at the point of slurry discharge.

CLASSIFYING CRYSTALLIZER EQUIPMENT AND PROCEDURE

The crystallizer used in this study was a mixed magma crystallizer having provisions for fines destruction, classified discharge, and clear liquor advance. The system studied was potassium chloride crystallized from a sodium chloride saturated brine. Design of the crystallizer followed closely the physical concepts implicit in the *R-z* crystallizer model. An elutriator for product removal was added to sharpen the classification range and to provide independent classification data for process modeling. Initial runs were made with a variable geometry removal port inside the mixed vessel which gave classification at the point of removal (see Figure 3*b*).

The crystallizer had a volume of 20 l and was constructed of epoxy fiberglass. The cooling assembly consisted of two concentric tight wound coils. The outer coil was welded to a stainless steel draft tube supported by three baffles. Agitation was achieved using a marine propeller with slurry flow either up or down the draft tube. Initial runs with removal port classification had flow up the draft tube; thereafter the flow was switched in a direction up the annular section. Temperature was controlled with a tempered water bath. Liquid level was maintained by clear liquor overflow withdrawn through the fines settler. Fines removal capability was achieved with a vertical annular baffled section between the inner and outer cooling coils. In addition to the clear liquor overflow, a peristaltic pump withdrew liquid from the top of the fines settler at a predetermined flow rate, thus carrying out the small crystals whose settling velocity was less than the upward flow velocity. Fines overflow was pumped through a steam heated coil to dissolve fine crystals. This stream was routed back to the crystallizer after passing through a precooler to remove excess heat. Product was removed through the bottom of the elutriator at a fixed rate of about 100 cm^3/min. Feed rate was fixed for each run at about 250 cm^3/min. The net volumetric difference between feed and product rates of about 150 cm^3/min overflowed through the fines settler back to the feed tank and resulted in a net increase in slurry density from the natural MSMPR value of about 60 to 80 g/l to 100 to 300 g/l. Slurry density and CSD in the crystallizer were measured directly by filtration of a sample removed from a sideport. CSD and slurry density were also measured for the product discharge.

Feed brine was recycled, heated, and reused for all data runs reported. The feed tank was molded from epoxy fiber glass and had a capacity of 50 gal. A donut shaped fiber glass divider split the tank into two sections. The bottom section was steam heated and was the compartment to which all returning streams entered. The crystallizer feed was withdrawn from the top section. Both sections were stirred by a single agitator with two propeller blades fitted to its shaft. A schematic process flow diagram for the classified crystallizer is shown in Figure 3*a*. The crystallizer temperature was kept at 32°C for all runs.

Initial runs used a feed liquor containing only potassium chloride dissolved in water. Brine analysis was simple, as only a chloride titration was necessary. However, instead of single, cubic crystals, the product contained excessive agglomerates and extensive castled growth. Such multicrystal growth is undesirable from a product standpoint as well as clouding the meaning of nucleation and growth rate kinetics.

A brief study of chemical additives was initiated to find a suitable habit modifier. A list of possible additives

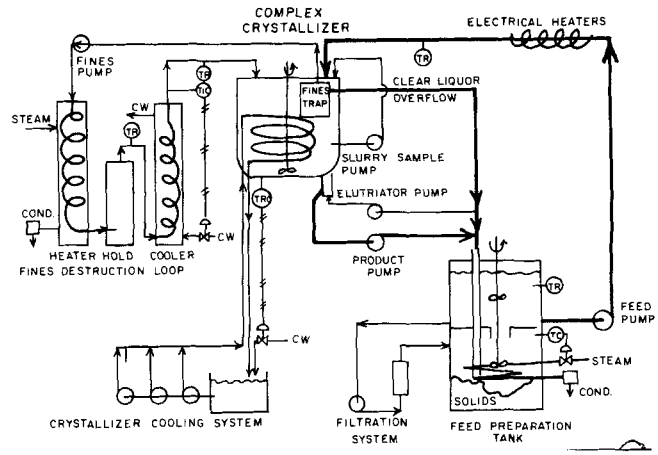

Fig. 3a. Schematic flow diagram of classified crystallizer.

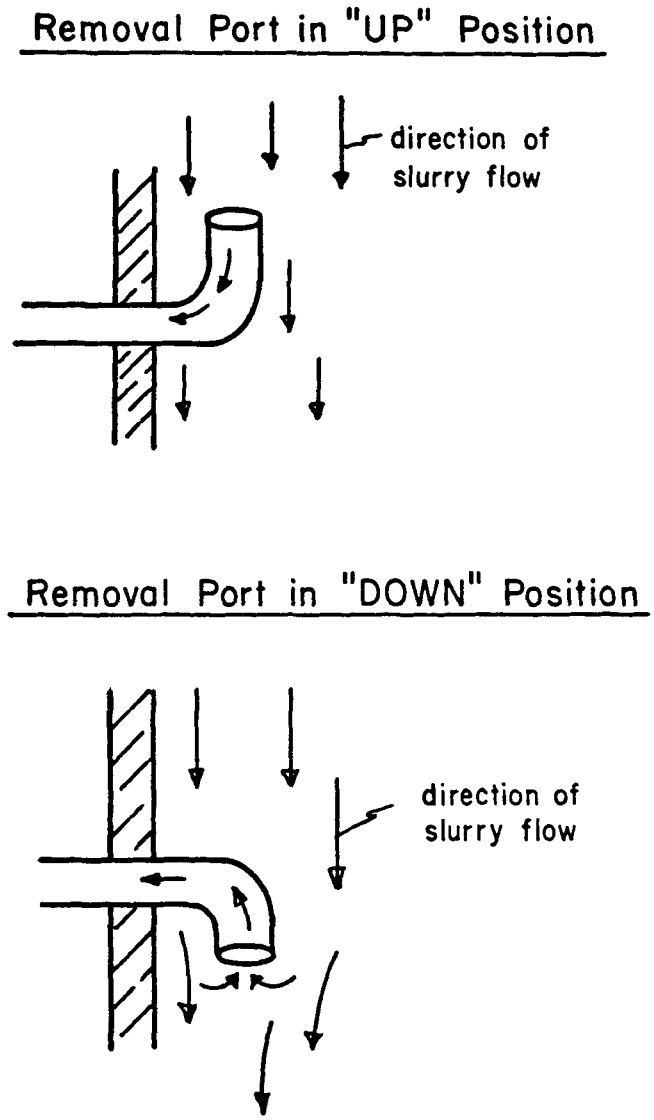

Fig. 3b. Removal port orientation for /74 runs.

was compiled from a knowledge of the chemical species present in an industrial potash crystallizer brine. Such brine constituents as carbonate, sulfates, borates and sodium ion were considered; however, only magnesium sulfate (0.75 mg/100 g water) and sodium chloride (near saturation) were actually added to the feed brine.

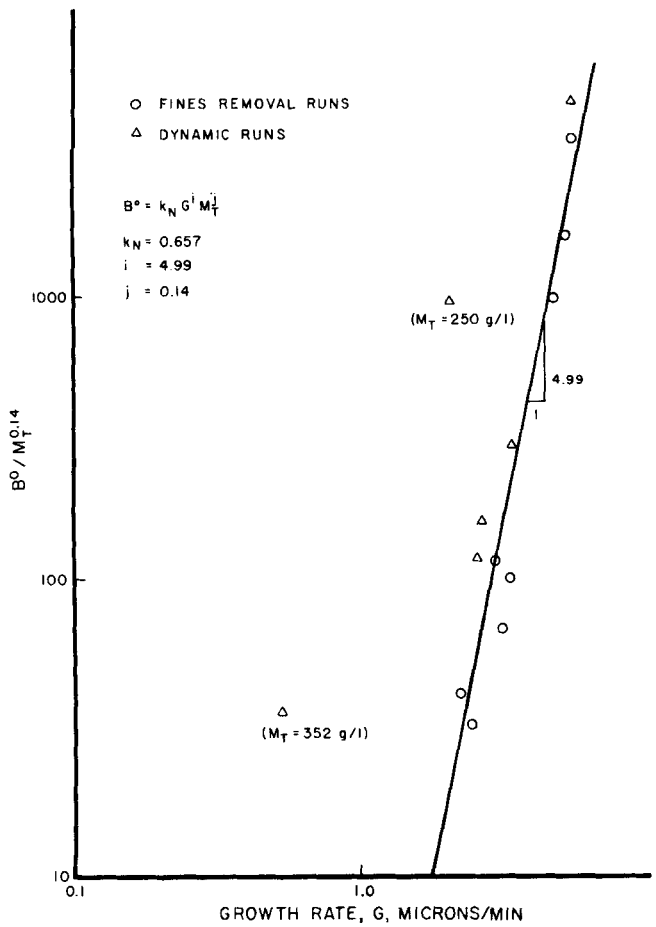

Fig. 4. Nucleation-growth rate kinetics correlation for the KCl system.

Noticeable improvement in crystal habit was found with such gross addition of sodium chloride. Single cubic crystals were present in large amounts in sizes up to approximately 400 μ. In the larger sizes agglomerates did appear, but the extent of agglomeration was not as severe as when sodium chloride was not present. Addition of magnesium sulfate did not significantly improve the crystal habit. But since magnesium and sulfate ions are present in industrial potash brines, it was decided to retain the magnesium sulfate in the liquor.

All runs were subsequently made with a liquor nearly saturated with sodium chloride and containing 0.75 g Mg/100 g water.

NUCLEATION AND GROWTH RATE KINETICS

Direct measurements of supersaturation were not made; thus, a kinetic growth constant relating growth rate and supersaturation was not obtained. Potassium chloride is a fast growing (class II) system, and a knowledge of the growth rate kinetics is not necessary to accurately model the system. It is sufficient to consider growth rate as constrained by a mass balance relating crystal production to crystal surface area. Both the mass balance constraint and a linear growth model ($G = k_g s$) were used in numerical simulations of the system. No significant differences in prediction of system behavior were observed using a value of k_g giving a 95% relief of supersaturation compared to the mass balance constraint (100% supersaturation relief).

Nucleation kinetics were obtained by sampling particle distributions in the fines dissolving loop. A small sample (about 100 cm^3) was diverted from this stream, quickly filtered on a porometric membrane, resuspended in conductive isopropanal solution, and counted with an electronic particle counter. Such particle population measurements in the 10 to 150 μm size range were taken during dynamic operation of the classified crystallizer as well as during steady state mixed removal operation. Even though the crystallizer was in a transient mode of operation, the CSD from the fines loop formed a quasi-equilibrium exponential distribution due to the small retention of the sizes affected by the dissolving system. These data could then be analyzed with conventional MSMPR data processing techniques. This observation has significant implications for the determination of nucleation kinetics from nonideal, real world crystallizers and will be exploited in future studies.

The nucleation and growth rate values obtained from analysis of fines loop CSD's were correlated in the conventional power law form as

$$B^o = k_N G^i M_T^j \qquad (7)$$

with the parameter values $i = 4.99$, $j = 0.14$, and $k_N = 0.657$. Figure 4 shows a correlation regression plot of these data fit to Equation (7). The data regressions were excellent except for two data points at very high slurry density ($M_T > 250$ g/l). These two points were omitted from the regression. Equation (7) fits the experimental nucleation data with an average deviation of 7.8%. This nucleation kinetics model was then used in computer simulations to predict CSD dynamics and instability.

EXPERIMENTAL RUNS

Experimental runs were conducted in three distinct phases; an early phase in which product classification and CSD instability was brought about by positioning of the internal removal port (runs labeled /74) and two latter phases where classification was achieved by an external elutriator and where the effect of fines removal was studied without product classification (runs labeled /76).

In the first set of runs before installation of the elutriator, operation with clear liquor advance indicated internal classification of the product stream at the removal port. Furthermore, this classification was of such magnitude as to make the crystal size distribution unstable. By rotating the removal port through 180 deg, so that the port pointed down instead of upward, classification was reduced enough to stabilize the CSD. These removal port configurations are shown in Figure 3*b*. In these runs, internal circulation was up through the draft tube and down the annulus; the flow pattern was subsequently reversed after installation of the elutriator classifier.

Two initial runs (runs 2/22/74 and 4/14/74) were made with the natural slurry density, that is, no clear liquor advance and no fines destruction. Both distributions were very nearly straight line MSMPR distributions. Thus, the removal port position had negligible effect on the CSD at low discharge solids concentration. In the presence of clear liquor advance CSD form and stability were found to depend solely on the direction in which the port was pointing, up or down. Thus the position of the removal port provided an on-off switch for CSD stability. Run pairs 3/10/74 and 3/28/74 were conducted under the same conditions except that for run 3/10/74 the removal port pointed up and for run 3/28/74 it pointed down. In both runs, the discharge slurry density was increased by clear liquor advance. Figure 5 shows the variation in discharge solids concentration for the two experiments. Run 3/28/74 maintained a constant value

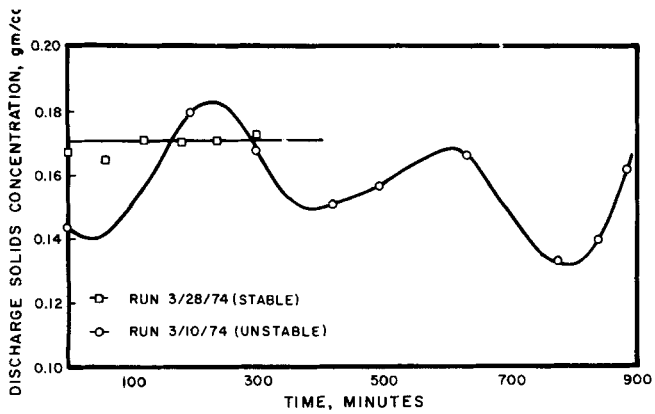

Fig. 5. Experimental product slurry density for stable and unstable run pair 3/28/74 and 3/10/74.

for slurry density of 0.17 g/ml. In run 3/10/74, a definite cycling of the solids concentration occurred. Figure 6 illustrates the cycles in run 3/10/74 of population density and weight fraction of particles of about 500 μ size as well as total discharge solids concentration.

In this run pair, the CSD was stable or unstable depending on the position of the removal port. In every case in which the removal port pointed down or when liquor advance was not present, the CSD was stable. Only those runs which had both liquor advance and the removal port pointing upward exhibited an unstable CSD. It is noted that clear liquor advance greatly decreases the product removal flow rate Q, thus exacerbating the classification effects due to removal port orientation.

Figure 7 shows the experimental CSD from run 7/15/76 with mixed withdrawal and fines removal. In this case, the removal port was positioned sideways and the direction of the agitator impeller was reversed, giving a more

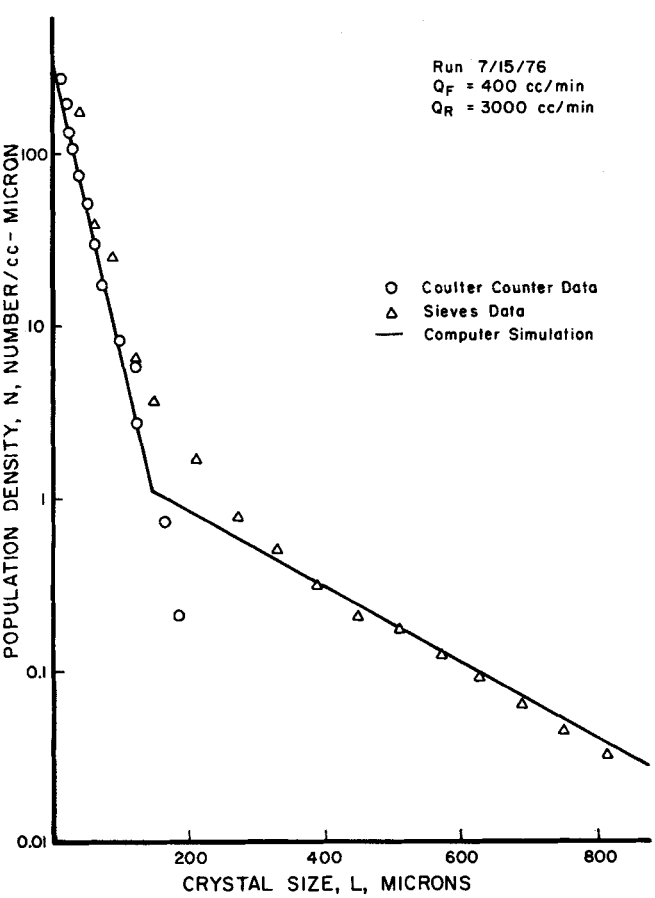

Fig. 7. Experimental crystal size distribution with mixed withdrawal and fines destruction.

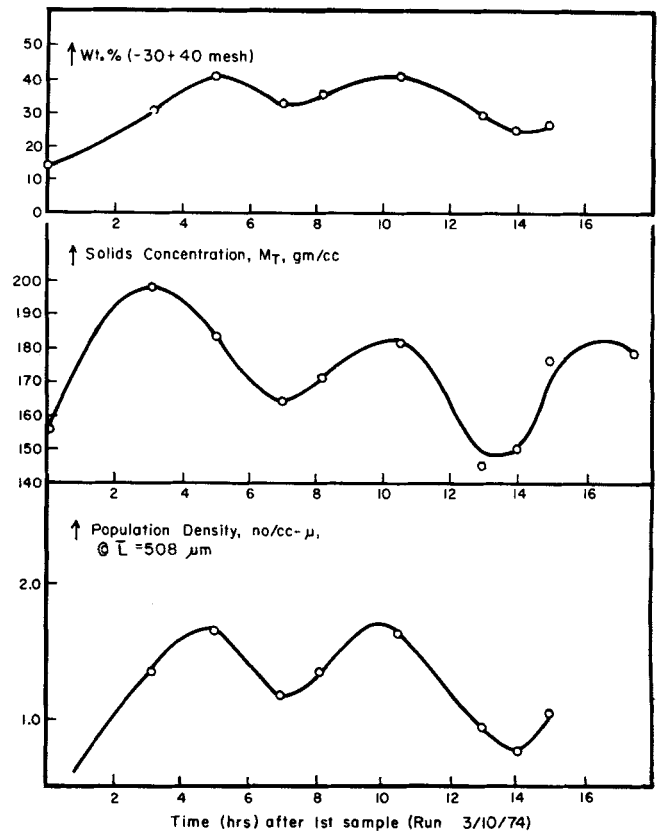

Fig. 6. Variation of crystal size distribution in unstable operation.

uniform slurry suspension at the point of withdrawal. No evidence of classification is apparent with this mode of operation as indicated by the straight population density plot of the product material. The slopes of these population density curves for the fines (particle counter data) and product (sieve data) are proportional to the fines and product removal rates, respectively, indicating equal and constant growth rate for both size ranges and

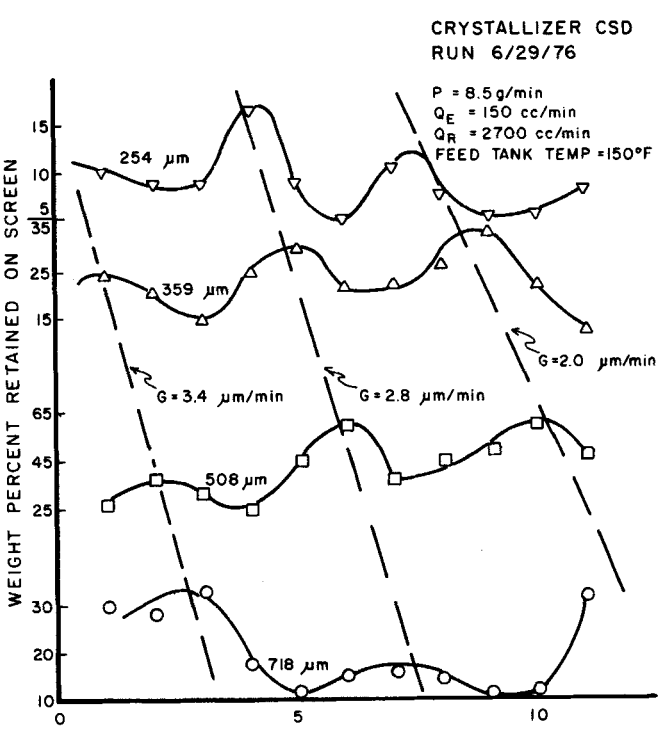

Fig. 8. Transient crystallizer crystal size distribution with unstable operation.

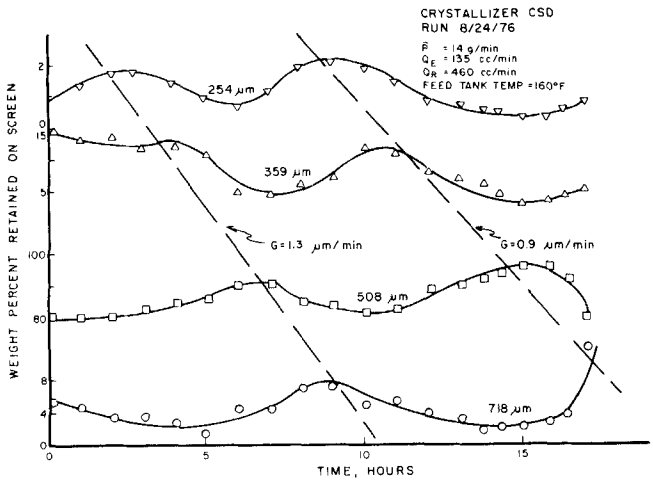

Fig. 9. Transient crystallizer crystal size distribution with unstable operation.

verifying the idealized fines dissolving CSD model. The solid line in Figure 7 was obtained by computer simulation of the run using experimentally measured process parameters and the nucleation kinetics of Equation (7).

The nucleation kinetics data shown in Figure 4 were obtained by extracting growth and nucleation rates from such straight line fines population density plots as shown by run 7/15/76, but under both classified and mixed product withdrawal conditions.

A final series of runs with an external elutriator product classifier was conducted to obtain extreme classification and to unambiguously verify the nonrepresentative product withdrawal mechanism of low-order CSD cycling. Figure 8 shows unstable crystallizer CSD data from run 6/29/76 using the product elutriator and a high fines destruction rate of about 3 l/min. Lines of constant growth rate of about 2 to 3.5 μ/min join CSD peaks in this figure. Figure 9 is a similar plot of unstable crystallizer CSD's for run 8/24/76 with a lower fines destruction rate of about 0.5 l/min. Lines of constant growth rate of about 1 μ/min join CSD peaks for this run, closely resembling the industrial data shown previously. Figure 10 shows unstable crystallizer CSD's from run 8/31/76 using a fines removal rate of about 1.4 l/min. Lines of growth rate of about 2 μ/min join CSD peaks for this run. Run 8/31/76 exhibited four CSD peaks before fouling. Note the increased cycle frequency and magnitude before fouling caused shutdown. Such a cycle change may have been caused by depletion of slurry density.

In all experimental runs with the classified crystallizer, operation was terminated after two to four cycles due to catastrophic fouling on the cooling coils. A critical slurry density of about 30 g/l was observed below which operation was impossible owing to extreme fouling. The nature of such fouling, which occurred near the end of each run, was such that suspension crystals less than about 200 to 300 μm were literally trapped from solution and attached as sandy agglomerates on cooling surfaces and process internals. Normal product removal of larger crystals then quickly dropped the slurry density to nil, thus terminating the run. Sustained CSD cycling could not be maintained in this apparatus with the current surface cooling arrangement; it was not feasible to modify the equipment for vacuum cooling or direct contact heat exchange.

Figures 11 and 12 well illustrate the wavelike nature of cycling CSD's as illustrated by run 8/31/76. Figure 11 is a population density plot showing the transient

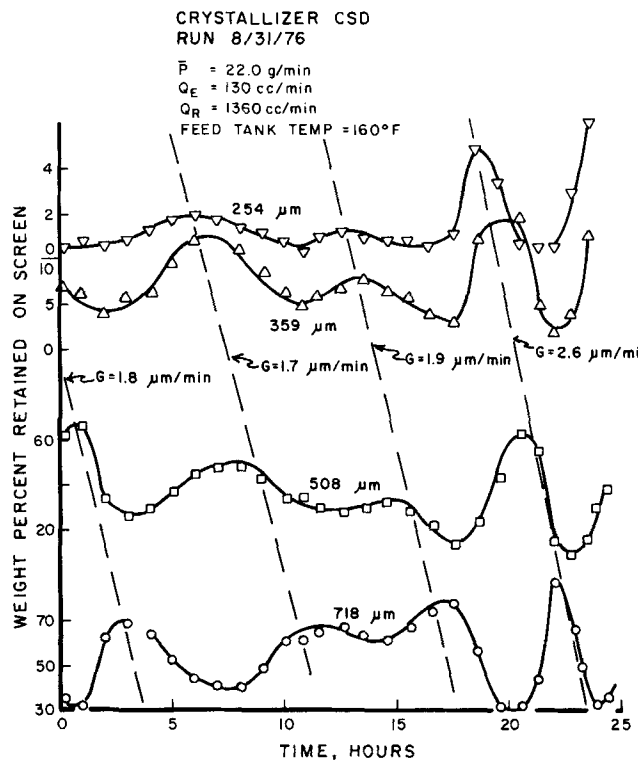

Fig. 10. Transient crystallizer crystal size distribution with unstable operation.

CSD's at different times from this run. Note the population peaks that march down the size axis with regular pattern. Figure 12 shows estimated peak CSD location micrometers vs. time for the same run. The average growth rate joining these peak locations is about 2 μm/min, but this value is seen to vary cyclically during the run. The bottom curve in Figure 12 shows the numerical derivative of peak location vs. time, again displaying the cyclical nature of the process. CSD cycle frequency was decreasing markedly toward the end of run 8/31/76, as seen in Figure 12, as well as in the raw CSD data (Figure 10) from this run.

Figure 13 shows transient crystallizer slurry density and net production rate from the elutriator for unstable run 8/31/76. Slurry density and production rate values result from the complex interaction of the elutriator with transient CSD's. Note that these values, although completely unstable, are not as uniformly cyclical as data with classification produced by removal port orientation. Sensitivity of elutriator performance to small perturbations in flow rate as well as the current CSD is indicated by these data. Note the catastrophic drop in slurry density (caused by internal fouling) which marks the end of the run.

ANALYSIS OF UNSTABLE CSD BEHAVIOR

The CSD behavior, both steady state and unstable, from this experimental study was thoroughly analyzed by computer simulation. The goals of this simulation phase were to verify the fines destruction/classification process model and to unequivocally demonstrate that product classification is the prime cause for the phenomena of low-order CSD cycling. Two complex generalized CSD dynamic simulators were used for this study, the Mark III CSD simulator (Nuttall, 1971) which had previously been developed and a new, more efficient simulator, Program CYCLER, developed in the present

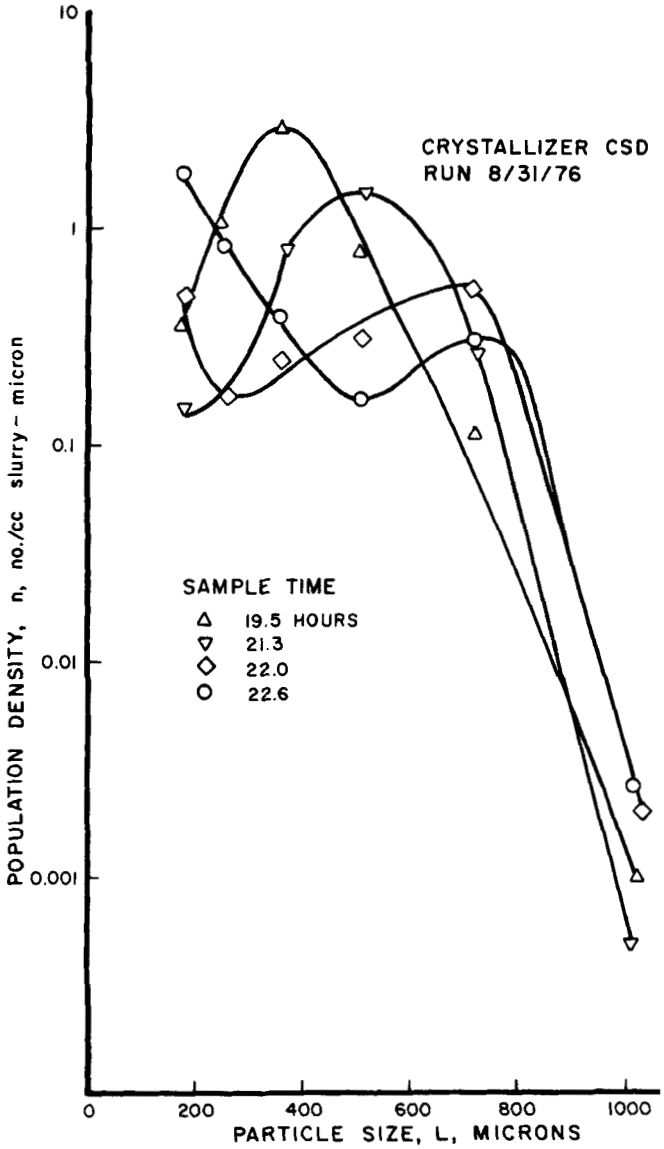

Fig. 11. Transient crystallizer population densities for unstable run.

study. The former CSD simulator uses a time-consuming explicit finite-difference formula (Heun method) to solve the transient population equation, while Program CYCLER uses a semianalytic algorithm in which the analytical solution to the piecewise constant coefficient, log population equation is iterated in time over periods in which the coefficients could be considered constant. Equivalent numerical results were obtained from both programs; however, the execution time of CYCLER was less than one tenth that of the Mark III program.

The modeling equations solved by the Mark III simulator are given as

$$\left.\begin{aligned} &\frac{\partial n}{\partial t}+\frac{\partial (Gn)}{\partial L}+\frac{n}{\tau}h(L)=0 \\ &n(0,t)=k_N G^{i-1}M_T{}^j \\ &G=\frac{P_I(t)}{\left(\frac{V}{2}\right)A(t)(\rho-C)} \end{aligned}\right\} \qquad (8)$$

where the internal production rate $P_I(t)$ includes mass dissolved and recrystallized in the fines destruction system. Program CYCLER solves a similar set of equations except the growth rate constraint in Equation (8) is replaced by a dynamic concentration balance coupled with a growth rate kinetics statement. Thus

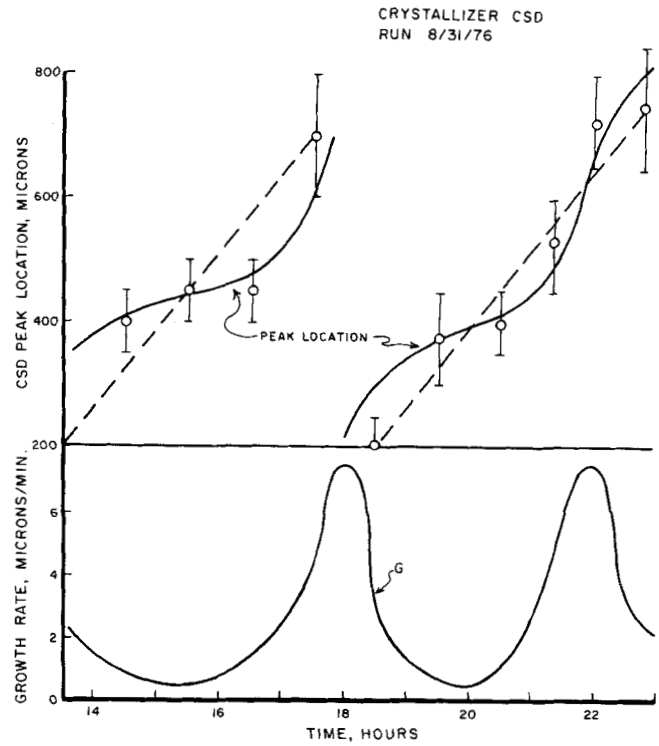

Fig. 12. Transient growth rates estimated by rate of change of peak location.

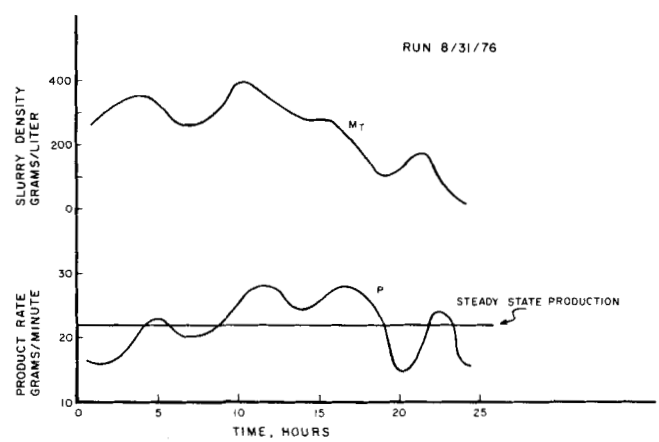

Fig. 13. Transient slurry density and production rate for unstable run.

$$\left.\begin{aligned} &G=\frac{P_I(t)-\epsilon V dC/dt}{\left(\frac{V}{2}\right)A(t)(\rho-C)} \\ &\text{together with} \\ &G=k_g[C-C_s] \end{aligned}\right\} \qquad (9)$$

When the value of the growth rate constant k_g was selected to give >95% relief of supersaturation, the stability predictions (stable or unstable, cycle period, cycle amplitudes, etc.) of both programs were essentially identical. Program CYCLER was used for the final analysis of all data reported in this study. This program and its numerical algorithm is described in detail in Part II of this paper.

The nucleation kinetics parameters i, j, and k_N were taken as measured from the fines destruction loop [Figure 4, Equation (7)]. The removal function $h(L)$ was set equal to the measured fines removal rate ratio R in the size range $(0, L_F)$ and to an experimentally measured classification function $C_P(L)$ for product sized crystals.

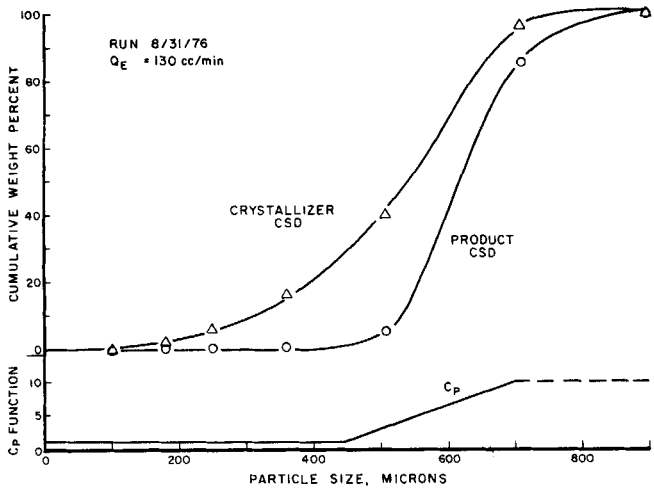

Fig. 14. Typical spread between crystallizer and product CSD's with elutriator operation.

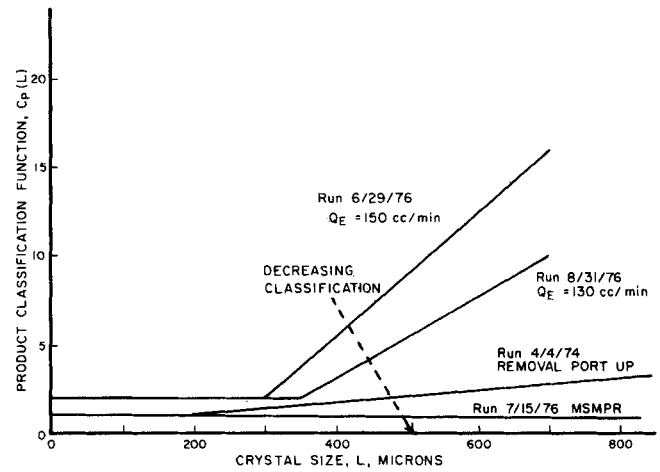

Fig. 15. Experimental product classification curves.

Other parameters that were fixed in the simulation were production rate, feed rate, and discharge rate, all as measured approximately in the experimental runs. The fines destruction size L_F was estimated from steady state CSD's with mixed withdrawal conditions, for example, Figure 8. It should be emphasized that no adjustable parameters were used in the simulation of these experimental data.

The classification function $C_P(L)$ was measured from a comparison of experimental suspension and product CSD's and was correlated with the following equation:

$$C_P(L) = \begin{cases} a & , L < L_p^- \\ a + (z-a)\dfrac{(L - L_p^-)}{(L_p^+ - L_p^-)} & , L \text{ in } (L_p^-, L_p^+) \\ z & , L > L_p^+ \end{cases} \tag{10}$$

The parameter a was as close to unity as would be expected for small sizes exhibiting negligible classification. Figure 14 shows typical product and crystallizer CSD's from run 8/31/76. The classification function was calculated from product and suspension CSD's (assuming ideal sampling of the latter) as

$$C_P \equiv \frac{n_P(L)}{n(L)} = \frac{M_T{}^P \Delta W^P(L)}{M_T \Delta W(L)} \tag{11}$$

where $W(L)$ is CSD expressed as cumulative weight fraction, and the superscript $(^P)$ refers to the product sample. Figure 15 shows experimental $C_P(L)$ functions for two elutriator flows and for the case of internal classification with an upward pointing removal port. The upper value z in the $C_P(L)$ parameterization depends very much on the current state of the CSD and was impossible to measure if a large fraction of oversize particles was not present at the time of sampling. [As $W(L) \to 1$ for large sizes, $\Delta W = \Delta W^P \to 0$, and the ratio of these quantities is impossible to evaluate.] In any event, the upper C_P value of z was reached at a size $L_p{}^+$, where $W(L_p{}^+) \approx 1$, and the particular value of z did not have much effect on system behavior. This is consistent with an earlier idealized classification theoretical study (Randolph et al., 1973) which showed that system stability was independent of z for all values $z > 5$.

In the case of the earlier runs with the upward pointing removal port, no internal crystallizer sample was taken, and no $C_P(L)$ function was measured. However, the fact that some classification was occurring at the discharge port was demonstrated at the end of stable run 4/4/74 by collecting product CSD's before and after a sudden reversal of the removal port. If we assume mixed removal with the port in the down position, the ratio of population densities upward port/downward port is a measure of the classification function C_P. These data from run 4/4/74 are shown in Figure 15 and were used in the simulation of run 3/10/74.

Table 1 summarizes the results of computer simulation for all of the experimental runs described in this paper. In all cases, stability was correctly predicted by the simulation using the measured parameters from each run with no adjustable parameters. Crystal growth rates (as estimated from peak displacement and/or the distribution in the fines loop) and cycle period were in reasonable agreement with the computer prediction.

CONCLUDING REMARKS

The unstable experimental runs reported in this paper together with the associated computer simulation unequivocally establish product classification as the principal cause of low-order CSD cycles, such as are observed in some large scale industrial crystallizers. The tendency towards cycling is increased with a large fines dissolving rate, but fines dissolving per se will not cause cycling; significant product classification must also be present. These data and the CSD simulation study confirm the validity of the so-called R-z crystallizer stability model (Randolph et al., 1973). Even though product classification is much less ideal than as described in the R-z model, the flavor of the problem is captured and the model is useful for a priori stability predictions.

Operation with the elutriator brought about severe product classification and conclusively illustrated the role of such classification in causing instability. However, most industrial crystallizers do not operate with external classifiers, although product removal is often far from representative. The experimental runs with the varying removal port orientation illustrate that such inadvertant classification at the removal port can be sufficient to cause CSD instability. The question arises: "What was the mechanism for product classification with the removal port in the up position?" Visual observations through the translucent fiber glass crystallizer indicated streaming of the larger particles towards the wall apparently due to the centrifuging action as the particles were thrown up and radially out of the draft tube. (This centrifuging action did not occur in the fines removal

Table 1. Summary of Experimental and Predicted Stability for Crystallizer Runs

Run	Experimental run parameters used in computer simulation					Stability		Cycle period, min		Time average growth rate, μm/min	
	L_F, μm	Q_F, l/min	Q_R, l/min	Q_S, l/min	L_c^-, μm	$(z-a)/(L_c^+ - L_c^-)$, $(\mu m)^{-1}$	Exp.	Simulation	Exp.	Simulation	Exp.	Simulation
3/28/74	100	0.212	1.22	—	—	—	Stable	Stable	—	—	1.1	1.5
2/22/74	—	0.217	—	—	—	—	Stable	Stable	—	—	1.68	1.7
4/4/74	—	0.216	—	—	—	—	Stable	Stable	—	—	1.25	1.7
3/10/74	100	0.222	1.04	—	200	0.0038	Unstable	Unstable	400	510	—	1.9
7/15/76	150	0.400	3.00	—	—	—	Stable	Stable	—	—	4.5*	4.8
6/29/76	90	0.285	2.70	0.150	300	0.0350	Unstable	Unstable	240	200	2.71	3.5
8/24/76	50	0.202	0.46	0.135	300	0.0320	Unstable	Unstable	390	270	1.31	2.1
8/31/76	60	0.250	1.36	0.130	450	0.0320	Unstable	Unstable	350	290	2.01	2.7

* From fines trap analysis.
† From sieve peak movement.

or elutriator runs where circulation was down through the draft tube.) Further classification occurred in the up removal port position as the removal flow was much lower than the streaming velocity of the particles; thus the larger crystals were jammed into the upward pointing removal tube.

The net effect of classification is to produce a narrower distribution of crystals with smaller average size, unless compensating increases are made in the fines dissolving rate. Thus, elimination of product classification could at the same time eliminate instability while increasing average particle size. However, a wider CSD would be produced.

An obvious way of stabilizing CSD cycling in an industrial crystallizer would be to promote mixing to better approach the ideal of mixed withdrawal. Such a change would almost certainly result in more fines and intermediate sizes produced in the form of a much wider distribution, even though the mean size might increase. An alternative approach would be to construct a feedback control system based on the current estimate of nuclei density. This information would then be used in regulation of the fines destruction rate. Part II of this study considers various feedback control schemes to stabilize CSD or at least minimize the effects of CSD swings.

Although considerable success was achieved in this study in the prediction of CSD stability as a function of CSD form, the work in no way represents a definitive study of the complex physical interactions of fines removal, classification, and clear liquor advance. However, once the form of the distribution was modeled, CSD stability was successfully explained with low-order nucleation kinetics experimentally obtained in the same system. Obviously, much more experimental work remains to be done to completely define individual process elements and their interaction with transient CSD's in order to a priori model the entire system.

NOTATION

- a = parameter in classification function
- $A(t)$ = specific crystal surface area in suspension
- B^o = nucleation rate
- C = solute concentration
- $C_P(L)$ = product classification function
- $G(t)$ = linear crystal growth rate
- $h(L)$ = size dependent crystal withdrawal function, $Q(L)/Q$ ($h = 1$ for MSMPR operation)
- i = exponent on G in power law nucleation kinetics expression
- $I(g)$ = stability boundary on $d(\log B^o)/d(\log G)$ for variable yield system.
- j = exponent on M_T in power law nucleation kinetics expression
- k_g = growth rate constraint coefficient
- k_N = proportionality rate constant in nucleation kinetics expression
- L = crystal size
- L_F, L_p = classification sizes for fines and product crystals
- M_T = solids concentration
- $n(L)$ = population density distribution function
- P = rate of make of crystals in suspension
- Q = mixed discharge flow rate
- $Q(L)$ = equivalent mixed discharge rate for crystals of size L
- R = ratio of fines removal to mixed discharge rate, $L < L_F$
- t = time
- V = suspension volume

w = cumulative weight fraction
z = ratio of oversize product discharge rate to mixed discharge rate, $L > L_p$

Subscripts

E = elutriator flow
F = crystal fines
i = inlet quantities
m = metastable limit
p = crystal product
R = fines loop flow
s = saturation

Greek Letters

β = fines dissolving factor, equal to ratio of mass dissolved to net production
ϵ = crystallizer void fraction
λ = fines dissolving exponential decay factor
ρ = crystal density
τ = mean retention time

Superscripts

$-$ = lower limit of z ramp function
$+$ = upper limit of z ramp function
P = product stream

ACKNOWLEDGMENT

The writers especially wish to acknowledge the efforts of Dr. Erroll Ottens, currently with Stork-Velsen, The Netherlands, who first assembled the classifying crystallizer apparatus and conducted the experimental runs with varying removal port orientation.

The principal investigator is grateful to Dr. Pawel Juzaszek of the Warsaw Technical Institute for his efforts in performing the Mark III CSD simulations. The Polish Educational Ministry is also acknowledged for their support of Dr. Juzaszek.

Appreciation is given to the National Science Foundation, Grants 36517X and ENG 75-04348 and to Kalium Chemicals, Ltd., for financial support of this work.

LITERATURE CITED

Hulburt, H. M., and D. G. Stefango, "Design Models for Continuous Crystallizers with Double Draw-off," *Chem. Eng. Progr. Symposium Ser. No. 95*, **65**, 50 (1969).

Lei, S., R. Shinnar, and S. Katz, "The Stability and Dynamic Behavior of a Continuous Crystallizer with a Fines Trap," *AIChE J.*, **17**, 1459 (1971).

Nuttall, H. E., "Computer Simulation of Steady-State and Dynamic Crystallizers," Ph. D. thesis, Department of Chemical Engineering, Univ. Ariz. (1971).

Randolph, A. D., and M. A. Larson, *Theory of Particulate Processes*, Chapt. 5, Academic Press, New York (1971).

Ibid., Chapt. 8.

Randolph, A. D., G. L. Beér, and J. P. Keener, "Stability of the Class II Classified Product Crystallizer with Fines Removal," *AIChE J.*, **19**, 1140 (1973).

Sherwin, M. B., R. Shinnar, and S. Katz, "Dynamic Behavior of the Well-Mixed Isothermal Crystallizer," *ibid.*, **13**, 1141 (1967).

Song, Y., and J. M. Douglas, "Self-Generated Oscillation in Continuous Crystallizers: Part II," *ibid.*, **21**, 924 (1976).

Manuscript received December 6, 1976; revision received April 22, and accepted April 27, 1977.

Crystal Size Distribution Dynamics in a Classified Crystallizer:

Part II. Simulated Control of Crystal Size Distribution

JAMES R. BECKMAN

and

ALAN D. RANDOLPH

Department of Chemical Engineering
University of Arizona
Tucson, Arizona 85721

Control of sustained limit-cycle instability in crystal size distribution (CSD) was simulated for a class II (high yield) crystallizer equipped with a fines destruction system and product classifier. Control was simulated by proportional control of nuclei density using fines destruction rate as the manipulated variable. The control constant necessary to eliminate instability was theoretically predicted and agreed with the constant found via simulation. Poorer control of CSD (inability to completely eliminate limit cycles) was predicted using slurry density and slurry withdrawal rate as the measured and manipulated variables, respectively. Development of techniques for fine crystal population measurements to estimate nuclei density are necessary for implementation of the former control scheme. The suggested nuclei density control scheme is effective both in minimizing CSD transients and for elimination of instability.

SCOPE

Some industrial class II crystallizers operating with fines destruction, clear liquor advance and product classification (the complex crystallizer) experience sustained limit-cycle behavior in crystal size distribution. As described in Part I of this series, both an industrial and a laboratory crystallizer producing potassium chloride were observed to develop cycling CSD's under certain operating conditions. Such unstable CSD behavior was not a result of outside disturbances but was caused by an interaction between nucleation rate and process configuration.

Control of sustained limit-cycle behavior in CSD is of industrial importance. Instability affects production by

Correspondence should be directed to Dr. Randolph. James R. Beckman is at the California State University, Northridge, California.